Supplementary information for

pH controllable photocurrent switching and molecular half-subtractor based on monolayer composite film of dinuclear Ru^{II} complex and graphene oxide

T. T. Meng[a], L. X. Xue[a], H. Wang[a], K. Z.Wang*[a], M. A. Haga*[b]

[a]*Beijing Key Laboratory of Energy Conversion and Storage Materials, College of Chemistry, Beijing Normal University, Beijing 100875, P.R. China. Fax: +86-10-58802075; Tel: +86-10-58805476/62209940; E-mail: kzwang@bnu.edu.cn (K.-Z.Wang)*
[b]*Department of Applied Chemistry, Faculty of Science and Engineering, Chuo University, 1-13-27 Kasuga, Bunkyo-ku, Tokyo 112-8551, Japan;E-mail: mhaga@kc.chuo-u.ac.jp (M.Haga)*

1. Experimental section

1.1 Materials

The GO suspensions were prepared by sonication of the graphite oxide prepared according to the modified Hummers method,[1] and purified by centrifugation and thorough dialysis as previously reported.[2] X-ray diffraction analysis of GO revealed a strong Bragg diffraction peak at 2θ of 12.2° yielding a *d*-spacing of 0.72 nm, which is in contrast to a much shorter layer-to-layer distance of 0.34 nm for graphite, and is consistent with reported values varying from~0.5 to 0.9 nm depending on the number of intercalated water molecules.[3] Synthesis and characterization of the dinuclear Ru(II) complex $[(bpy)_2Ru(HL^1)Ru(H_2L^2)]^{4+}$ **Ru1**$^{4+}$ {where bpy = 2,2'-bipyridine, HL^1 = 2-(4-(2,6-di(pyridin-2-yl)pyridin-4-yl)phenyl and H_2L^2 = 2,6-bis(benzimidazol-2-yl)pyridine} will be published in a separate paper.

1.2 Instrumentation

UV-visible absorption spectra were recorded on a GBC Cintra 10e UV-visible spectrophotometer using quartz substrate. All of the photoelectrochemical and cyclic voltammetry measurements were carried out at room temperature in 0.1 M aqueous Na_2SO_4 solution on a CHI electrochemical analyser using an indium-tin oxide (ITO) coated glass substrate modified with the self-assembled films, which had an effective area of 0.28 cm^2, a saturated calomel electrode (SCE) and a Pt wire as the working, reference and counter electrodes, respectively. The polychromatic light irradiation (730 nm > λ > 325 nm) used for the photoelectrochemical studies was produced by a 500 W xenon lamp fitted with an infrared cut-off filter. The distance between the lamp and the electrode was approximately 15 cm. To acquire the photocurrent action spectrum, a monochromatic light was obtained from a 500 W xenon lamp (Changtuo Photoelectronic Technology Ltd., Beijing, PR China) fitted with a certain additional bandpass filter with the spectral width of ± 5 nm. The monochromatic light intensities were measured with a light gauge radiometer, which is corrected by standard silicon cells (FZ-A, Photoelectric Instrument Factory of Beijing Normal University).

2. Method for deriving HOMO and LUMO energy levels

In order to get insight into the photocurrent switching mechanism,the energies of relavent electronic states involved in the redox reactions occurring for photocurrent switching have to be known. The absolute energies in eV for the highest occupied molecular orbital or the lowest empty molecular orbital (E_{HOMO} or $_{LUMO}$) and the 0–0 transition energy E^{00} are derived according to Eqs (1) and (2), by using an energy of −4.74 eV for SCE with respect to the zero vacuum level.[4]

E_{HOMO} or $_{LUMO} = -4.74 - E_{onset}$ (ox) or E_{onset} (red) (1)

$E^{00} = E_{LUMO} - E_{HOMO} = 1240/\lambda_{onset}$ (2)

where λ_{onset} is the onset absorption wavelength in nm; E_{onset} (ox) or E_{onset} (red) is onset oxidation or reduction potential in V vs. SCE, in which -E_{onset} (ox) or -E_{onset} (red) corresponds to relative HOMO or LUMO energies. The relative HOMO or LUMO energies in V vs. SCE can be converted into the absolute energies in eV and vice versa. By taking experimentally observed λ_{onset} values of 544 and 579 nm, E_{HOMO} values of +0.67 and +0.31 V vs SCE for **Ru1** aqueous solution of pH 1.00 and 10.0, respectively, the corresponding E_{LUMO} values of -1.61 and -1.84 V vs SCE were derived. For highly n-doped semiconductors with high conductivity such as ITO, it is reasonable to assume that the Fermi level coincides with the conduction band edge (E_{CB} = -4.5 eV), while its valence band top was reported to locate at E_{VB} = -8.3 eV.[5] The reduction potentials of O_2 which normally was treated as electron acceptor as it could accept an electron to form a superoxide anion, was taken to be -0.50 V vs. SCE.[6] Fermi and conduction band energy levels of GO were taken to be +0.16 V vs SCE (-4.9 eV)[7] and -0.76 V vs. SCE,[8] respectively.

References

1. W. S. Hummers and R. E. Offeman, *J. Am. Chem. Soc.*, 1958, **80**, 1339.
2. Y. C. Dai, W. Yang, X. Chen, L. H. Gao and K. Z. Wang, *Electrochim. Acta*, 2014, **134**, 319.
3. Y. Q. Qian, A. Vu, W. Smyrl and A. Steina, *J. Electrochem. Soc.*, 2012, **159**, A1135.
4. K. Z. Wang, L. H. Gao, G. Y. Bai, L. P. Jin and C. H Huang, *Inorg. Chem.*, 2002, **41**, 3353.
5. L.Sereno, J. J. Silber, L. Otero, M. del Valle Bohorquez, A. L. Moore, T. A. Moore and D. Gust, *J. Phys. Chem.,* 1996, **100**, 814.
6. H. Imahori, H. Norieda, Y. Nishimura, I. Yamazaki, K. Higuchi, N. Kato, T. Motohiro, H. Yamada, K. Tamaki, M. Arimura and Y. Sakata, *J. Phys. Chem. B,* 2000,**104**, 1253.
7. T. F. Yeh, F. F. Chan, C. T. Hsieh and H. Teng, *J. Phys. Chem. C,* 2011, **115**, 22587.
8. T. Cassagneau, J.H. Fendler, S.A. Johnson, T.E. Mallouk, *Adv. Mater.,* 2000, **12**, 1363.

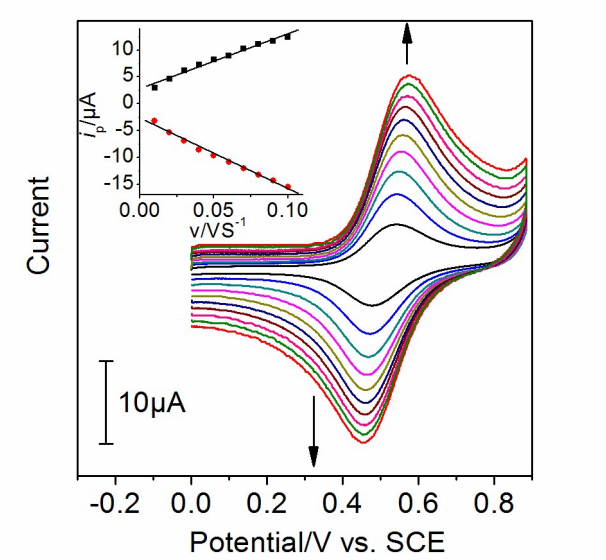

Fig. S1 Cyclic voltammograms of ITO/(GO/**Ru1**)$_1$ film in 0.1 M aqueous Na_2SO_4 solution of pH 7.0 at different scan rates from 0.01 V/s to 0.1 V/s.

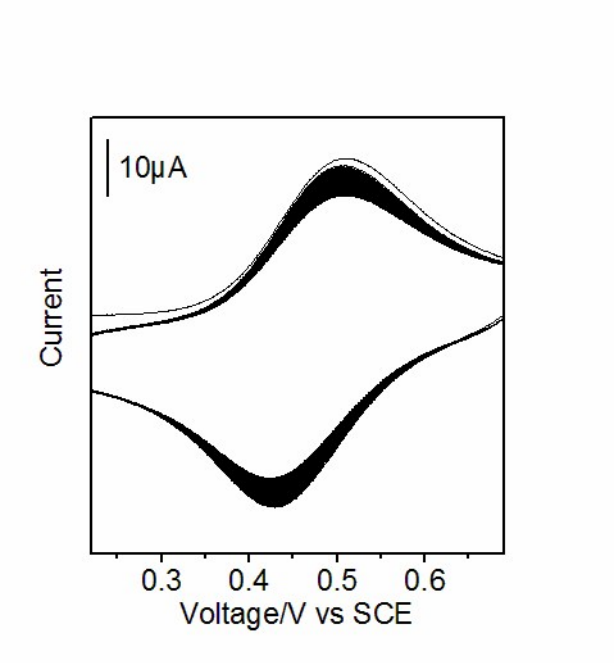

Fig. S2 CV profiles of ITO/(GO/**Ru1**)$_1$ film recorded at 100 mV/s with 50 continuous scans from 0 to 1 V vs SCE in 0.1 M Na_2SO_4 aqueous solution of pH 7.0.

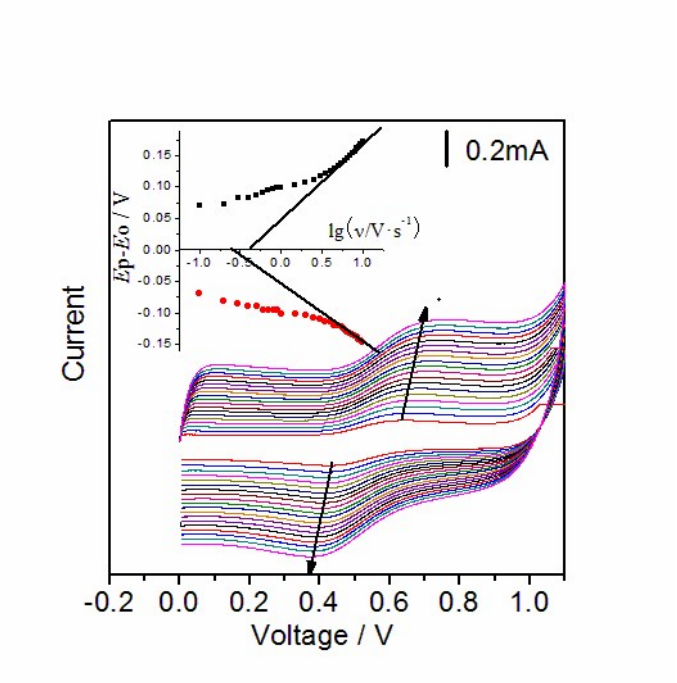

Fig. S3 Cyclic voltammograms of ITO/(GO/**Ru1**)$_1$ film in BR buffer solution of pH 7.0 upon increasing the scan rate (ν) from 0.10 V/s to 10.0 V/s, with shifting directions of the peak potentials being shown by arrows. The inset shows the dependence of the overpotentials on lgν.

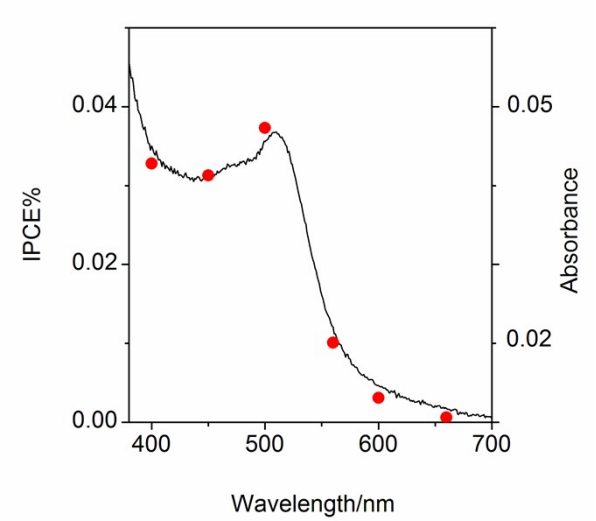

Fig. S4 Comparison of the photocurrent action spectrum (red dots) with the visible absorption spectrum (black line) of (GO/**Ru1**)$_1$-modified ITO electrode in $NaClO_4$ aqueous solution as biased at -0.4 V vs. SCE.

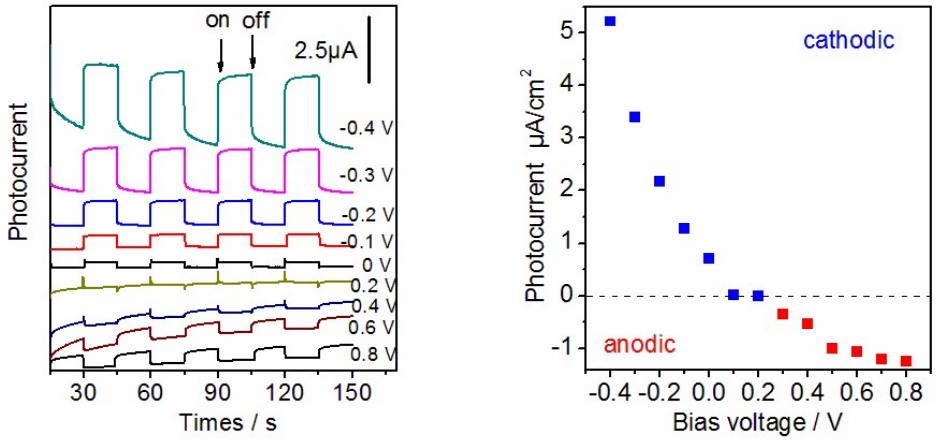

Fig. S5 Left panel: photocurrent responses induced by switching on and off the light irradiation of the $(GO/\mathbf{Ru1})_1$ film in 0.1 M Na_2SO_4 aqueous solution at pH 7.0, which was biased at potentials of -0.4, -0.3, -0.2, -0.1, 0, +0.2, +0.4, +0.6 and +0.8 V vs. SCE under a white light irradiation of 100 mW cm^{-2} (area of the electrode ≈ 0.28 cm^2). Right panel: a plot of photocurrents vs. biased potentials.

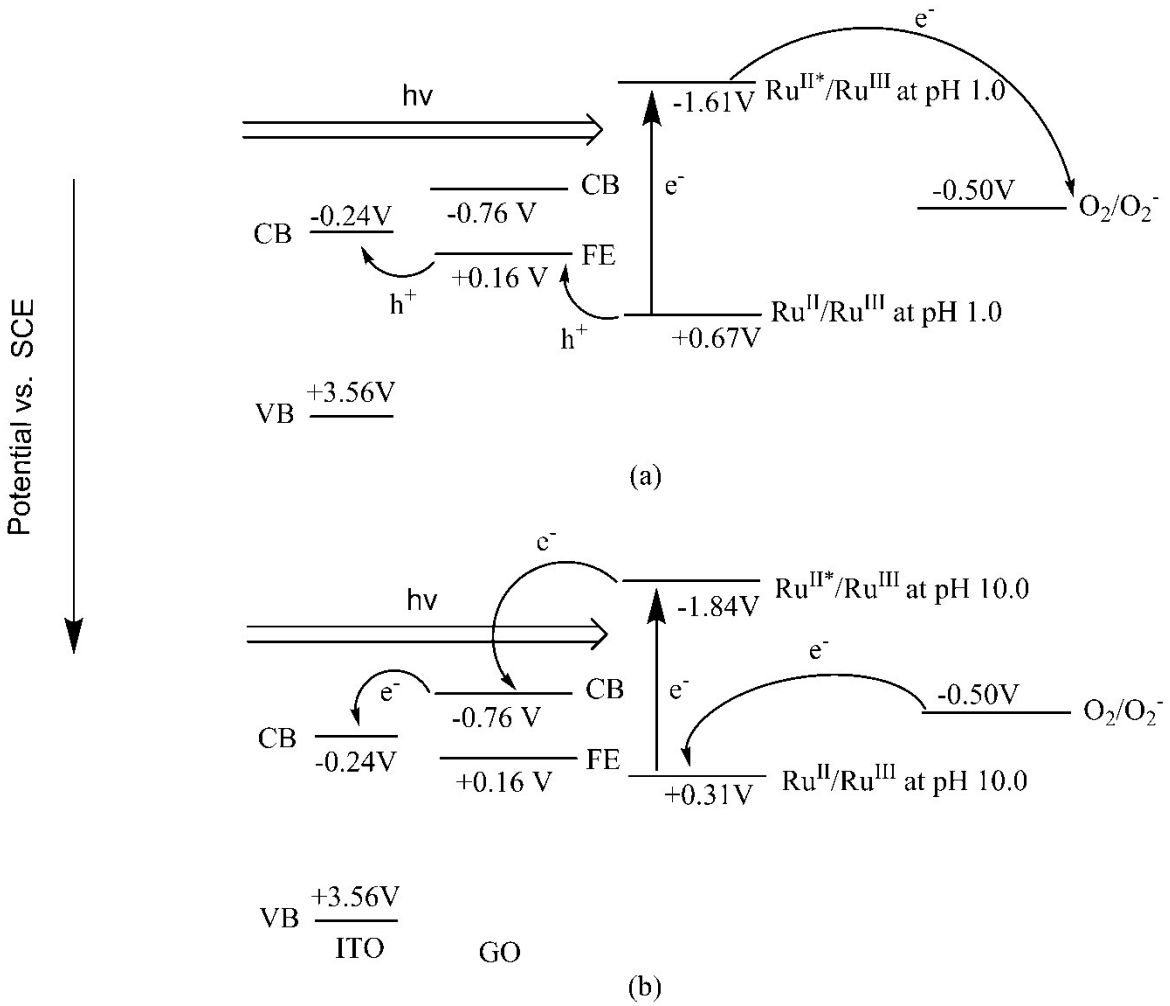

Fig. S6 Energy level alignments for cathodic (a) and anodic (b) photocurrent generation involving conduction band (CB) and vaclence band (VB) of ITO, Fermi energy level (FE) and conduction band of GO, ground-state oxidation potential (HOMO) and excited-state oxidation potential (LUMO) of **Ru1**$^{4+}$, and redox potential of redox mediators O_2/O_2^-.

Input		Output
pH	Bias potential	$\lvert I_{ph} \rvert$
I_1	I_2	O_2
0(pH 7)	0(0.0V)	1(109 nA)
0(pH 7)	1(0.1V)	0(24 nA)
1(pH 8)	0(0.0V)	0(53 nA)
1(pH 8)	1(0.1V)	0(66 nA)

Input		Output
pH	Bias potential	PD
I_3	I_4	O_1
0(pH 2)	0(0.4V)	0(83 nA)
0(pH 2)	1(0.5V)	1(-115 nA)
1(pH 3)	0(0.4V)	1(-110 nA)
1(pH 3)	1(0.5 V)	1(-176 nA)

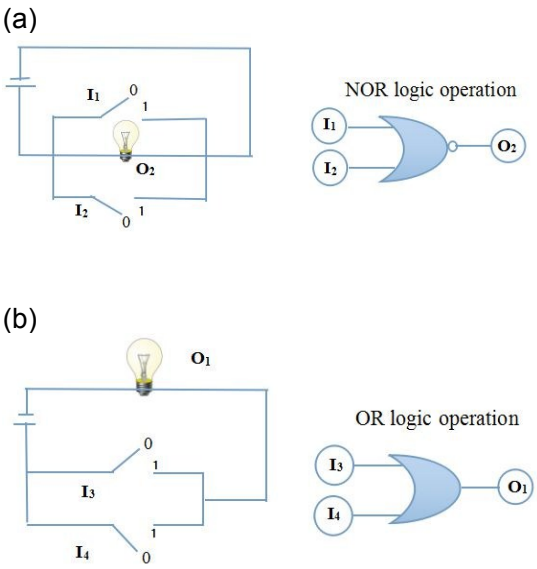

Fig. S7 The truth tables (left) and representations of the electronic circuit (middle) and combinational logic scheme (right) of NOR (a) and OR (b) logic operations generated from monolayer ITO/(GO/**Ru1**)$_1$ film.

(a)

Inputs		Output
$[H^+]$ I_5	Bias potential I_6	| *I*ph | O_2
0(10^{-6} M)	0(0.1 V)	0(48 nA)
0(10^{-6} M)	1(0.2 V)	1(127 nA)
1(10^{-5} M)	0(0.1 V)	1(143 nA)
1(10^{-5} M)	1(0.2 V)	0(62 nA)

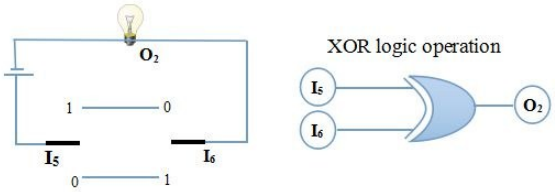

(b)

Inputs		Output
$[H^+]$ I_5	Bias potential I_6	PD O_1
0(10^{-6} M)	0(0.1 V)	0(48 nA)
0(10^{-6} M)	1(0.2 V)	1(-127 nA)
1(10^{-5} M)	0(0.1 V)	0(143 nA)
1(10^{-5} M)	1(0.2 V)	0 (62 nA)

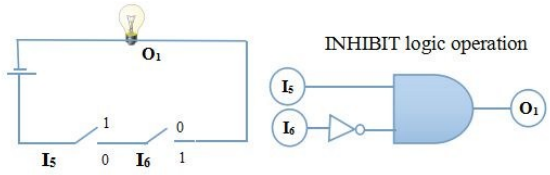

Fig. S8 The truth tables (left) and representations of the electronic cir combinational logic scheme (right) of XOR (a) and INHIBIT (b) logic operation

Table S1. Electron transfer rate constant at different pH condition.

pH	v_a	v_c	α
2	0.6636	0.2150	0.5108
3	0.7919	0.4847	0.6203
4	0.7819	0.3643	0.6821
5	0.5380	0.2974	0.6440